Molecular orientation induced by high−speed substrate transfer during vacuum vapor deposition of organic films

Toshinori Matsushima and Hideyuki Murata*

School of Materials Science, Japan Advanced Institute of Science and Technology,

1-1 Asahidai, Nomi, Ishikawa 923-1292, Japan

ABSTRACT

The authors investigate a relationship between substrate transfer speeds during vacuum vapor deposition and orientation characteristics of organic molecules. Results show that rod−shaped molecules of alpha−sexithiophene (α−6T) are oriented in a substrate transfer direction and an absorption dichroic ratio of 1.44 is obtained from the oriented α−6T molecule film when a high substrate transfer speed of 4 m s^{-1} is used. By combining the substrate transfer technique with homoepitaxial growth of α−6T molecules on a rubbed surface, the absorption dichroic ratio further increases to 4.29. Polarized electroluminescence (EL) characteristics are

investigated using rod−shaped molecules of 4,4′−bis[4−(di−p−tolylamino)styryl]biphenyl (DPAVBi) as a light−emitting hole−transport layer. An EL dichroic ratio of 2.12 is obtained due to an orientation of DPAVBi molecules caused by combining two techniques.

* Corresponding author. Tel.: +81 761 51 1531; fax: +81 761 51 1149

E-mail address: murata-h@jaist.ac.jp (H. Murata)

Keywords:

Organic light−emitting diodes

Molecular orientation

Substrate transfer during vacuum deposition

Polarized absorption and fluorescence spectra

Homoepitaxial growth on rubbed surface

1. Introduction

Recently, organic light−emitting diodes (OLEDs) have gained tremendous attention for use in full color flat panel displays and solid−state lighting. For OLEDs based on small molecules, multilayer structures are adopted to improve electron−to−photon conversion efficiencies and operational durability and are constructed by successive deposition of organic and metal layers from multiple deposition sources in a vacuum apparatus [1]. Organic layers embedded in OLEDs are generally vacuum−deposited on stationary substrates at deposition rates less than 0.1 nm s^{-1} unless substrates are moved to make layer thickness uniform. If the multilayer OLED structure can be constructed on a high−speed transferred substrate (for example, 1 m s^{-1}) at an extremely high deposition rate (for example, 1 μm s^{-1}) using a reel−to−reel manufacturing process, the overall cost (tact time) must be reduced to manufacture the OLEDs. The deposition rates and the substrate transfer speeds for the reel−to−reel manufacturing process are considered the key factors affecting performances of OLEDs. Indeed, it has been demonstrated that electron mobilities of tris(8−hydroxyquinoline)aluminum (Alq_3) are reduced and power consumption of OLEDs is significantly increased by a small increase in deposition rate of Alq_3 from 0.2 to 0.7 nm s^{-1}

[2,3]. In contrast, there has been still a lack of understanding of a relationship between substrate transfer speeds during vacuum deposition and characteristics of organic films and OLEDs. In this study, we discuss results for a change in these characteristics caused by the high−speed substrate transfer during the vacuum deposition.

The schematic structure of the vacuum evaporator used in this study is shown in Fig. 1(a). Our specially designed vacuum evaporator is equipped with a reel having a diameter of ≈12 cm, which can be rotated in a vacuum. Cleaned substrates are mechanically fixed onto the peripheral part of the reel. Organic films are vacuum−deposited on the substrates being transferred at a certain speed. The substrate transfer speeds can be controlled from 0 to 4 m s^{-1} by changing the reel rotation speeds from 0 to 666 rpm. In this study, we investigate how the substrate transfer speeds and molecular lengths affect polarized absorption, fluorescence, and electroluminescence (EL) characteristics of organic films using the above−mentioned evaporation system, which is modeled on the reel−to−reel manufacturing process. We demonstrate that rod−shaped molecules such as alpha−sexithiophene (α−6T) and 4,4′−bis[4−(di−p−tolylamino)styryl]biphenyl (DPAVBi) are oriented in the substrate transfer

direction to some extent when a high substrate transfer speed of 4 m s^{-1} is used during the film deposition. Moreover, we find that the combination of the high−speed substrate transfer with homoepitaxial growth of organic molecules on a rubbed surface is a very effective technique used to obtain highly oriented organic molecule films. There have been many techniques to induce molecular orientations, such as mechanical orientations [4−8], liquid−crystalline self−organization [9−13], Langmuir−Blodgett deposition [14−16], and orientations on a specific substrate [17−20], details of which are reviewed in Ref. 21. Besides these techniques, the high−speed substrate transfer technique to induce a molecular orientation is believed to open an alternative way for unique anisotropic characteristics of various organic electronic devices, such as polarized EL [6,11,13,15−17,19] and enhanced charge−carrier conduction [5,7,12,14,18] when the reel−to−reel process is used to manufacture the devices.

2. Experimental

The chemical structures of organic molecules used in this study are shown in Fig. 1(a). Molecules of Alq_3, *N*–*N*′−diphenyl−*N*−*N*′−bis(1−naphthyl)−1,1′−biphenyl−4,4′−diamine

(α-NPD), α−6T, and DPAVBi with different molecular lengths were used for comparison. High−purity source materials of Alq_3 (Nippon Steel Chemical), α−NPD (Nippon Steel Chemical), and DPAVBi (Luminescence Technology) were purchased and used as−received. A source material of α−6T was purchased from Aldrich and purified twice using a temperature−gradient vacuum train sublimation technique prior to use. Optically polished fused silica substrates were cleaned using ultrasonication in acetone, followed by ultrasonication in detergent, pure water, and isopropanol. Then, the substrates were further cleaned in an ultraviolet−ozone treatment chamber for 30 min. The cleaned substrates were placed on the reel surface inside the evaporation chamber [see Fig. 1(a)]. The chamber was evacuated to a base pressure of $\approx 1\times10^{-4}$ Pa. 20 nm films of Alq_3, α−NPD, α−6T, and DPAVBi were vacuum−deposited from temperature−controlled carbon crucibles on the cleaned substrates being transferred by rotating the reel. The substrate transfer speed was set at either 0.1, 1, 2, 3, or 4 m s^{-1} during the film deposition. The deposition rate of the organic films was set at 0.007 nm s^{-1} unless otherwise mentioned. The deposition rate and the final film thickness were controlled using a calibrated quartz crystal microbalance (QCM) installed near the rotation reel. It is noted that the substrate passes above the evaporators repeatedly

during the organic deposition, the situation of which is different from that of the actual reel−to−reel process. The polarized absorption and fluorescence spectra of the films were measured respectively using an absorption spectrometer (V670, JASCO) and a fluorescence spectrometer (FP−6500, JASCO) equipped with a single optical polarizer when an electric field vector of polarized light is parallel and perpendicular to the substrate transfer direction. The excitation light wavelengths for the fluorescence spectra were 350 nm for α−NPD and 400 nm for Alq_3, α−6T, and DPAVBi. There was an error of ≈2% for absorbances and fluorescence intensities obtained in this study probably due to slight time instability of excitation light intensities and photodetector sensitivities during the optical measurements. Surface morphologies and structural characteristics of the films were evaluated using an atomic force microscope (AFM) (SPA400, Seiko Instruments) and an X−ray diffractometer (XRD) (M18XHF, MAC Science).

To investigate the polarized EL characteristics, four types of OLEDs based on a bilayer structure of DPAVBi and MPT were fabricated using the substrate transfer speed (r) of 0.1 or 4 m s^{-1} during the DPAVBi deposition: (A) glass substrate/ITO (150 nm)/DPAVBi (70 nm)

(r=0.1 m s^{-1})/MPT (200 nm)/LiF (0.5 nm)/Al (100 nm), (B) glass substrate/ITO (150 nm)/DPAVBi (70 nm) (r=4 m s^{-1})/MPT (200 nm)/LiF (0.5 nm)/Al (100 nm), (C) glass substrate/ITO (150 nm)/rubbed DPAVBi/DPAVBi (70 nm) (r=0.1 m s^{-1})/MPT (200 nm)/LiF (0.5 nm)/Al (100 nm), and (D) glass substrate/ITO (150 nm)/rubbed DPAVBi/DPAVBi (70 nm) (r=4 m s^{-1})/MPT (200 nm)/LiF (0.5 nm)/Al (100 nm). The OLED structures are illustrated in Fig. 1(b). The ITO and the MPT stand for indium tin oxide as an anode layer and 2,4−bis−biphenyl−4−yl−6−(4′−pyridin−2−yl-biphenyl−4−yl)−[1,3,5]triazine as a wide−energy−gap electron−transport layer [22], respectively. High−purity source materials of MPT (TOSOH), LiF (Nacalai Tesque), and Al (Nilaco) were used as−received. The glass substrates coated with the 150 nm ITO anode layer having a sheet resistance of 10 Ω sq^{-1} (Sanyo Vacuum Industries) were cleaned in the way similar to those mentioned before. For the devices (A) and (B), a 70 nm DPAVBi layer was vacuum−deposited as a light−emitting hole−transport layer on the cleaned ITO substrate at the substrate transfer speed of 0.1 (A) or 4 m s^{-1} (B). On the other hands, a 20 nm DPAVBi buffer layer was first vacuum−deposited on the ITO layer at the substrate transfer speed of 0.1 m s^{-1}. This layer was rubbed 250 times with a dust−free nylon cloth inside a nitrogen−filled glove box to orient DPAVBi molecules

along the rubbing direction [23]. To fabricate the devices (C) and (D), an additional 70 nm DPAVBi layer was vacuum−deposited on the rubbed surface at the substrate transfer speed of 0.1 (C) or 4 m s^{-1} (D). Then, a 200 nm MPT electron−transport layer, a 0.5 nm LiF electron−injection layer [24], and a 100 nm Al cathode layer were successively vacuum−deposited on the DPAVBi layers to complete the devices (A)−(D). While the layers of MPT, LiF, and Al were evaporated, the substrates were made stationary to investigate the influence of the substrate transfer speeds on molecular orientation characteristics of DAPVBi only. The film deposition rates were set at 0.007 nm s^{-1} for DAPVBi, 0.1 nm s^{-1} for MPT, 0.01 nm s^{-1} for LiF, and 0.5 nm s^{-1} for Al. The active device area was defined at 3.125 mm^2 by an overlapped area of the ITO layer and the Al layer. The completed devices were encapsulated using a glass cap and an ultraviolet curing epoxy resin together with a desiccant sheet. The device preparation was conducted without exposing the devices to air. The polarized EL spectra were measured through an optical polarizer using a photonic multichannel analyzer (C7473, Hamamatsu Photonics) when the devices were operated at a current density of 10 mA cm^{-2}. The current density−voltage−external quantum efficiency characteristics of the devices were measured using a computer−controlled sourcemeter (2400,

Keithley) and an integrating sphere installed with a calibrated silicon photodiode.

3. Results and discussion

3.1. Orientation of α−6T molecules by high−speed substrate transfer

The polarized absorption and fluorescence spectra of the 20 nm α−6T film prepared at the substrate transfer speed of 4 m s^{-1} are shown in Fig. 2(a). The shapes of the polarized spectra parallel and perpendicular to the substrate transfer direction are similar. However, the polarized spectrum parallel is larger in absorbance than that perpendicular, indicating that a long axis of α−6T molecules is aligned to the substrate transfer direction to some extent. The absorption and fluorescence dichroic ratios (D_{AB} and D_{FL}) are estimated to be almost same values (1.44 and 1.46, respectively) from the differences in peak absorbance and fluorescence intensity between the polarized spectra parallel and perpendicular.

The absorption peaks in this wavelength range originate from π−π* transition of α−6T having an electronic transition dipole moment along its long molecular axis [23,25−27]. The sharp absorption peak at ≈360 nm and the weak side absorption peaks located in a

wavelength range from 400 to 600 nm are assigned to aggregated and unaggregated molecules, respectively [23,26,27]. The observation of the optical dichroism in the whole wavelength range indicates orientations of both aggregated and unaggregated molecules along the substrate transfer direction by the high−speed substrate transfer.

Polarized absorption spectra were measured when α−6T thicknesses (L) were changed from 2 to 5, 10, 15, and 20 nm. The absorption dichroic ratios estimated from their polarized absorption spectra are independent of the film thicknesses: D_{AB}=1.40 (L=2 nm), D_{AB}=1.43 (L=5 nm), D_{AB}=1.42 (L=10 nm), D_{AB}=1.41 (L=15 nm), and D_{AB}=1.44 (L=20 nm), indicating that the in−plane molecular orientation caused by the substrate transfer is not changed significantly in the thickness direction of the α−6T films.

The 20 nm α−6T films are prepared on the fused silica substrates at the substrate transfer speeds of 0.1, 1, 2, 3, and 4 m s^{-1} to measure their polarized absorption and fluorescence spectra. The relationship between the dichroic ratios calculated from the polarized spectra and the substrate transfer speeds is shown in Fig. 2(b). Both absorption and

fluorescence dichroic ratios follow the same curves. The dichroic ratios in the substrate transfer speed range from 0.1 to 2 m s^{-1} are ≈1.00, but the dichroic ratios gradually increase from ≈1.00 to ≈1.40 as the substrate transfer speeds are increased from 2 to 4 m s^{-1}. This observation indicates that the higher substrate transfer speeds during the film deposition are essential to induce the molecular orientation.

It has been reported that a standing orientation of α−6T molecules is dominant on a hydrophilic fused silica substrate [26,27]. Since unpolarized absorbances (≈0.056 at a wavelength of 360 nm) of the α−6T films are independent of the substrate transfer speeds, the standing orientation is not changed significantly. Thus, we assume that the substrate transfer mainly induces the change in in−plane orientation of originally lying molecules in the transfer direction.

The orientation order parameter (*S*) is used to evaluate the degree of the molecular orientation. The orientation order parameter is given by the equation [28,29],

$$S = \frac{D_{AB} - 1}{D_{AB} + 2}. \quad (1)$$

If the orientation order parameter is 0, molecules are in−plane random in a film. If the orientation order parameter is 1, molecules are perfectly oriented in a certain direction. This evaluation is possible only in the in−plane direction. The relationship between the calculated orientation order parameters and the substrate transfer speeds is also shown in Fig. 2(b). We find that α−6T molecules are in−plane random in the substrate transfer speed range between 0.1 and 2 m s^{-1}, but the molecular orientation is gradually enhanced as the substrate transfer speeds are increased from 2 to 4 m s^{-1}. When the substrate transfer speed is 4 m s^{-1}, the orientation order parameter of the α−6T film is calculated to be 0.128. The maximum substrate transfer speed is 4 m s^{-1} for our vacuum evaporator. We suggest that use of substrate transfer speeds higher than 4 m s^{-1} further enhances the molecular orientation.

3.2. Relationship between molecular lengths and orientations

The 20 nm films of Alq_3, α−NPD, and DPAVBi are vacuum−deposited on the fused silica substrates at the substrate transfer speed of 4 m s^{-1} and their polarized absorption and fluorescence spectra are measured and compared. There is no optical dichroism from the films of Alq_3 [Fig. 3(a)] and α−NPD [Fig. 3(b)]. On the other hands, the absorption dichroic

ratios of the films of α−6T [Fig. 2(a)] and DPAVBi [Fig. 3(c)] are obtained and calculated to be 1.44 and 1.24, respectively. These results suggest that rod shapes of molecules such as α−6T and DPAVBi are required to induce the molecular orientations by the high−speed substrate transfer while relatively spherical−shaped molecules such as Alq_3 and α−NPD are in−plane random in the films.

AFM images and XRD patterns of the films of Alq_3, α−NPD, DPAVBi, and α−6T prepared on the fused silica substrates at the substrate transfer speed of 4 m s^{-1} were measured. Results show that all films have grain structures having the grain diameters of ≈100 nm for α−6T and ≈30 nm for the other films. The average surface roughnesses (*R*a) measured from a 1×1 μm^2 area are 0.37±0.07 nm for Alq_3, 0.36±0.04 nm for α−NPD, 0.32±0.08 nm for DPAVBi, and 3.65±0.17 for α−6T. There is no obvious changes in surface morphology and in grain shape along the substrate transfer direction. Moreover, the films exhibit no clear diffraction peaks, indicating rather little crystallization.

A 20 nm α−NPD film was first vacuum−deposited on the fused silica substrate at the

substrate transfer speed of 0.1 m s^{-1}. Then, a 20 nm α−6T or DPAVBi film was vacuum−deposited on the first deposited α−NPD film at the substrate transfer speed of 4 m s^{-1} to investigate the molecular orientation characteristics of α−6T and DPAVBi on the random α−6T molecule film. Since measured absorption spectra of these bilayer samples correspond to the sum of α−NPD absorption and α−6T absorption (or DPAVBi absorption), the absorption spectrum of the pure 20 nm α−NPD film shown in Fig. 3(b) was subtracted from the absorption spectra of the bilayer samples to calculate the absorption dichroic ratios of α−6T and DPAVBi. The absorption dichroic ratios thus calculated are 1.35 for α−6T and 1.17 for DPAVBi, which are slightly smaller than those measured from α−6T and DPAVBi prepared directly on the fused silica substrates, maybe due to imperfect calculative subtraction caused by light reflection and/or light scattering, but provide clear evidence that molecules of α−6T and DPAVBi are surely oriented on random α−NPD molecules using the high−speed substrate transfer technique.

When the deposition rates of α–6T were changed from 0.07 to 0.007 and 0.0007 nm s^{-1}, a change in orientation order parameter of 20 nm α–6T films prepared at the substrate transfer

speed of 4 m s^{-1} was investigated. As the deposition rates are decreased from 0.07 to 0.007 and 0.0007 nm s^{-1}, the orientation order parameters are found to increase from 0.071 to 0.128 and 0.140. Molecule speeds in gases are described by conventional Maxwell–Boltzmann distribution and the most probable speed (v_m) of molecules is given by

$$v_m = \sqrt{\frac{2kT}{m}} \quad , \tag{2}$$

where k is the Boltzmann constant, T is the thermodynamic temperature, and m is the molecular mass of a gas. The most probable speeds of α-6T and DPAVBi are calculated to be 132 and 110 m/s, respectively using their molecular masses and crucible temperatures. These calculated values are much higher than the substrate transfer speeds used in this study. Thus, we assume that the molecular orientation occurs during a surface migration process of molecules because the decrease in deposition rate is expected to cause an increase in surface migration time. After molecules evaporated from an evaporator arrive at a substrate surface, molecules are known to migrate on the substrate surface for a certain period of time [30]. When a substrate transfer speed is sufficiently higher than a surface migration speed of molecules during the surface migration process, molecules would be dragged on the transferred substrate surface, resulting in the molecular orientation. The detailed mechanism

of the molecular orientation induced by the high–speed substrate transfer (especially for rod–shaped molecules) is not clearly understood, but is now under investigation.

3.3. Combination of substrate transfer with homoepitaxial film growth

It has been shown that it is possible to obtain highly oriented organic molecule films by homoepitaxial film growth on a rubbed layer [17,31–34]. Here, we demonstrate that the combination of the high–speed substrate transfer technique with the homoepitaxial film growth technique further enhances the molecular orientation characteristics. First, a 20 nm α–6T buffer film deposited on the fused silica substrate at the substrate transfer speed of 0.1 m s^{-1} is rubbed 15 times using a nylon cloth in a given direction [23]. The rubbing induces a decrease in absorbance of ≈74% when compared with the as–deposited α–6T film. The absorption dichroic ratio of the rubbed α–6T film is measured to be 3.12 from its polarized absorption spectra. Second, an additional 20 nm α–6T film is homoepitaxially grown on the rubbed surface. The substrate transfer speed during the homoepitaxial growth is set at 0.1 or 4 m s^{-1}. The rubbing direction corresponds with the substrate transfer direction. The surface morphologies of the homoepitaxially grown films are confirmed to be similar to those of the

substrate–transferred films.

Whereas the result obtained in this study reveals that α–6T molecules are in–plane random in the film prepared at the low substrate transfer speed of 0.1 m s^{-1} [see Fig. 2(b)], the α–6T film prepared on the rubbed surface at the same speed exhibits the large polarization of absorption and fluorescence due to the homoepitaxial growth effect [Fig. 4(a)]. The estimated absorption dichroic ratio and the orientation order parameter of this homoepitaxially grown film are 3.82 and 0.485, respectively. When the 20 nm α–6T film is homoepitaxially grown on the rubbed surface at the high substrate transfer speed of 4 m s^{-1}, the molecular orientation is further enhanced, leading to the absorption dichroic ratio of 4.29 and the orientation order parameter of 0.523 [Fig. 4(b)].

The features of the absorption spectra of the homoepitaxially grown α–6T films markedly differ from those of the absorption spectra of the substrate–transferred α–6T films. The ≈360 nm absorption peak decreases in absorbance for the homoepitaxially grown films (Figs. 4(a) and 4(b)) when compared with the substrate–transferred films (Fig. 2(a)),

somehow indicating a decrease in component of aggregated α–6T molecules under the homoepitaxial growth. Moreover, the maximum unpolarized absorbances (intermediate values between the polarized absorbances parallel and perpendicular) of the homoepitaxially grown films (Figs. 4(a) and 4(b)) are much larger than those of the substrate–transferred films (Fig. 2(a)), indicating that the homoepitaxial growth induces an increase in the number of lying molecules relative to standing molecules.

The similar techniques of the substrate transfer and the homoepitaxial growth are conducted on the DPAVBi films. A reduction in absorbance of ≈85% and an absorption dichroic ratio of 1.56 are observed when rubbing a 20 nm DPAVBi buffer film 250 times. An additional 20 nm DPAVBi film is homoepitaxially grown on the rubbed DPAVBi surface at the substrate transfer speed of 0.1 or 4 m s^{-1}. The optical measurements reveal that the absorption dichroic ratio and the orientation order parameter are 1.95 and 0.240, respectively, for the DPAVBi film prepared on the rubbed surface at the low substrate transfer speed of 0.1 m s^{-1} [Fig. 5(a)]. The absorption dichroic ratio and the orientation order parameter further increase to 2.39 and 0.317, respectively, when the high substrate transfer speed of 4 m s^{-1} is

used during the homoepitaxial growth [Fig. 5(b)].

3.4. Polarized electroluminescence

The average surface roughnesses and the fluorescence quantum efficiencies of the films of α–6T and DPAVBi are compared to determine which material is more suitable for the OLED application. The average surface roughness of the DPAVBi film (≈0.32 nm) is about 11 times smaller than that of the α–6T film (≈3.65 nm), preventing an electrical short circuit under operation of OLEDs. Moreover, the fluorescence quantum efficiency of the DPAVBi film (18±1%) is about 36 times higher than that of the α–6T film (0.5±0.1%) [35], enhancing external quantum efficiencies of OLEDs. Owing to the smaller surface roughness and the relatively higher fluorescence quantum efficiency, DPAVBi is chosen as a light–emitting hole–transport layer to fabricate the devices (A)–(D) (see the device structures in Fig. 1(b)).

The drive voltages and external quantum efficiencies of the devices (A)–(D) operated at a current density of 10 mA cm^{-2} are summarized in Table 1. The EL spectra of the devices (A)–(D) operated at a current density of 10 mA cm^{-2} are shown in Fig. 6. The drive voltages

and external quantum efficiencies of the devices (A)–(D) are nearly same, indicating that the rubbing process does not degrade the overall device performance. There is no EL from the MPT electron–transport layer, meaning that the EL spectra completely originate from electrically excited DPAVBi molecules. It is expected that electrons and holes injected from the electrodes recombine near the DPAVBi/MPT interface. The EL dichroic ratio (D_{EL}) of 1.11 is observed from the device (B) prepared using the high substrate transfer speed of 4 m s^{-1} whereas the device (A) prepared at the low substrate transfer speed of 0.1 m s^{-1} exhibits the EL dichroic ratio of 1.00 (see Table 1). The use of the homoepitaxial film growth on the rubbed DPAVBi surface increases the EL dichroic ratio to 1.78 for the device (C). The combination of the high–speed substrate transfer technique with the homoepitaxial film growth technique further increases the EL dichroic ratio to 2.12 for the device (D). This tendency of the observed EL dichroic ratios is in good agreement with that of the fluorescence dichroic ratios discussed before. It should be pointed out that the effect of the substrate transfer is smaller than that of the homoepitaxial film growth for the molecular orientation. However, we can conclude that the combination of the substrate transfer technique with the homoepitaxial growth technique is useful to obtain polarized EL from highly oriented

molecule films.

4. Conclusion

We investigate changes in molecular orientation characteristics caused by high–speed substrate transfer during film deposition using a special vacuum evaporator modeled on a reel–to–reel manufacturing process. From results obtained in this study, we find that: (1) a long axis of organic molecules is oriented along a substrate transfer direction, (2) the molecular orientation is enhanced as substrate transfer speeds are increased, (3) rod shapes of molecules are essential to induce the molecular orientation by the high–speed substrate transfer, (4) combination of the high–speed substrate transfer with homoepitaxial film growth on a rubbed surface is an effective technique for the molecular orientation, and (5) polarized EL is observed from oriented molecules by combining two techniques. We assume that the molecular orientation occurs during a surface migration process of molecules because the molecular orientation is affected by deposition rates. We believe that the high–speed substrate transfer technique is advantageous to manufacture sophisticated organic electronic devices, such as OLEDs showing polarized EL and organic thin–film transistors showing enhanced

charge–carrier mobilities in a certain direction, if much higher substrate transfer speeds and patterned substrates are used to further enhance the molecular orientation.

Acknowledgement

The authors are grateful to Tokyo Research Laboratory, TOSOH Corporation and Frontier Materials Chemistry Group, Sagami Chemical Research Center for providing us with MPT, an electron–transport material. This work is supported by Grants–in–Aid for Scientific Research (Grant Nos. 21760005, 20241034, and 20108012). Part of this work is based on "Development of the next generation large–scale organic EL display basic technology (Green IT Project)" contracted with New Energy and Industrial Technology Development Organization (NEDO). This research is supported by the Japan Society for the Promotion of Science (JSPS) through its "Funding Program for World-Leading Innovative R&D on Science and Technology (FIRST Program).

References

[1] C. W. Tang, S. A. VanSlyke, Appl. Phys. Lett. 51 (1987) 913.

[2] B. J. Chen, W. Y. Lai, Z. Q. Gao, C. S. Lee, S. T. Lee, W. A. Gambling, Appl. Phys. Lett. 75 (1999) 4010.

[3] H. Mu, H. Shen, D. Klotzkin, Solid–State Electron. 48 (2004) 2085.

[4] D. D. C. Bradley, R. H. Friend, H. Lindenberger, S. Roth, Polymer 27 (1986) 1709.

[5] P. Dyreklev, G. Gustafsson, O. Inganäs, H. Stubb, Solid State Commun. 82 (1992) 317.

[6] P. Dyreklev, M. Berggren, O. Inganäs, M. R. Andersson, O. Wennerström, T. Hjertberg, Adv. Mater. 7 (1995) 43.

[7] S. Nagamatsu, W. Takashima, K. Kaneto, Y. Yoshida, N. Tanigaki, K. Yase, Appl. Phys. Lett. 84 (2004) 4608.

[8] M. Campoy–Quiles, Y. Ishii, H. Sakai, H. Murata, Appl. Phys. Lett. 92 (2008) 213305.

[9] J. H. Wendroff, G. Lüssem, R. Festag, A. Greiner, C. Schmidt, C. Unterlechner, W. Heitz, Adv. Mater. 7 (1995) 923.

[10] A. P. Davey, R. G. Howard, W. J. Blau, J. Mater. Chem. 7 (1997) 417.

[11] H. Tokuhisa, M. Era, T. Tsutsui, Appl. Phys. Lett. 72 (1998) 2639.

[12] M. Redecker, D. D. C. Bradley, M. Inbasekaran, E. P. Woo, Appl. Phys. Lett. 74 (1999)

1400.

[13] A. Liedtke, M. O'Neill, A. Wertmöller, S. P. Kitney, S. M. Kelly, Chem. Mater. 20 (2008) 3579.

[14] J. Paloheimo, P. Kuivalainen, H. Stubb, E. Vuorimaa, P. Yli–Lahti, Appl. Phys. Lett. 56 (1990) 1157.

[15] V. Cimrová, M. Remmers, D. Neher, G. Wegner, Adv. Mater. 8 (1996) 146.

[16] A. Bolognesi, G. Bajo, J. Paloheimo, T. Östergärd, H. Stubb, Adv. Mater. 9 (1997) 121.

[17] M. Era, T. Tsutsui, S. Saito, Appl. Phys. Lett. 67 (1995) 2436.

[18] Z. Bao, A. J. Lovinger, A. Dodabalapur, Appl. Phys. Lett. 69 (1996) 3066.

[19] H. Yanagi, S. Okamoto, Appl. Phys. Lett. 71 (1997) 2563.

[20] A. Borghesi, A. Sassella, R. Tubino, S. Destri, W. Porzio, Adv. Mater. 10 (1998) 931.

[21] M. Grell, D. D. C. Bradley, Adv. Mater. 11 (1999) 895.

[22] T. Matsushima, M. Takamori, Y. Miyashita, Y. Honma, T. Tanaka, H. Aihara, H. Murata, Org. Electron. 11 (2010) 16.

[23] T. Matsushima, H. Murata, Appl. Phys. Lett. 98 (2011) 253307.

[24] L. S. Hung, C. W. Tang, M. G. Mason, Appl. Phys. Lett. 70 (1997) 152.

[25] D. Fichou, G. Horowitz, B. Xu, F. Garnier, Synth. Met. 48 (1992) 167.

[26] H.–J. Egelhaaf, P. Bäuerle, K. Rauer, V. Hoffmann, D. Oelkrug, Synth. Met. 61 (1993) 143.

[27] Y. Kanemitsu, N. Shimizu, K. Suzuki, Y. Shiraishi, M. Kuroda, Phys. Rev. B 54 (1996) 2198.

[28] R. D. B. Fraser, J. Chem. Phys. 24 (1956) 89.

[29] R. D. B. Fraser, J. Chem. Phys. 29 (1958) 1428.

[30] A. Kubono, N. Yuasa, H.−L. Shao, S. Umemoto, N. Okui, Appl. Surf. Sci. 193 (2002) 195.

[31] Y. Tomioka, S. Imazeki, Thin Solid Films, 210-211 (1992) 352.

[32] T. Kanetake, K. Ishikawa, T. Hasegawa, T. Koda, K. Takeda, M. Hasegawa, K. Kubodera, H. Kobayashi, Appl. Phys. Lett. 54 (1989) 2287.

[33] J. C. Wittmann, P. Smith, Nature, 352 (1991) 414.

[34] H. Tanaka, T. Yasuda, K. Fujita, T. Tsutsui, Adv. Mater. 18 (2006) 2230.

[35] Fluorescence quantum efficiencies of films of α–6T and DPAVBi are measured using integrating sphere system (C9920, Hamamatsu Photonics).

Table 1. Drive voltages, external quantum efficiencies, and EL dichroic ratios of OLEDs (A)–(D) operated at 10 mA cm^{-2}.

Device	Deposition condition of DPAVBi		Drive Voltage [V]	External quantum efficiency [%]	EL dichroic ratio
	Rubbed DPAVBi layer	Substrate transfer speed [m s^{-1}]			
(A)	w/o	0.1	10.6±0.1	0.28±0.02	1.00
(B)	w/o	4	10.1±0.1	0.27±0.01	1.11
(C)	w	0.1	10.4±0.2	0.28±0.03	1.78
(D)	w	4	10.4±0.2	0.27±0.02	2.12

Figure captions

Fig. 1. (a) Illustration of vacuum evaporator and chemical structures of organic molecules used in this study. Rotation reel is installed inside evaporator to control substrate transfer speeds. (b) Illustration of OLED structures where DPAVBi layers are deposited at substrate transfer speeds of 0.1 m s^{-1} [(A) and (C)] and 4 m s^{-1} [(B) and (D)].

Fig. 2. (a) Polarized absorption and fluorescence spectra of 20 nm α–6T film prepared on fused silica substrate at substrate transfer speed of 4 m s^{-1} and (b) changes in absorption and fluorescence dichroic ratios and orientation order parameters as function of substrate transfer speeds. D_{AB}, D_{FL}, and S stand for absorption dichroic ratio, fluorescence dichroic ratio, and orientation order parameter, respectively.

Fig. 3. Polarized absorption and fluorescence spectra of 20 nm films of (a) Alq_3, (b) α–NPD, and (c) DPAVBi prepared on fused silica substrates at substrate transfer speed of 4 m s^{-1}.

Fig. 4. Polarized absorption and fluorescence spectra of 20 nm α–6T films prepared on 15 times rubbed α–6T surfaces at substrate transfer speeds (*r*) of (a) 0.1 and (b) 4 m s^{-1}.

Fig. 5. Polarized absorption and fluorescence spectra of 20 nm DPAVBi films prepared on 250 times rubbed DPAVBi surfaces at substrate transfer speeds (*r*) of (a) 0.1 m s^{-1} and (b) 4 m s^{-1}.

Fig. 6. Polarized EL spectra of devices (A)–(D) operated at current density of 10 mA cm^{-2}. D_{EL} stands for electroluminescence dichroic ratio.

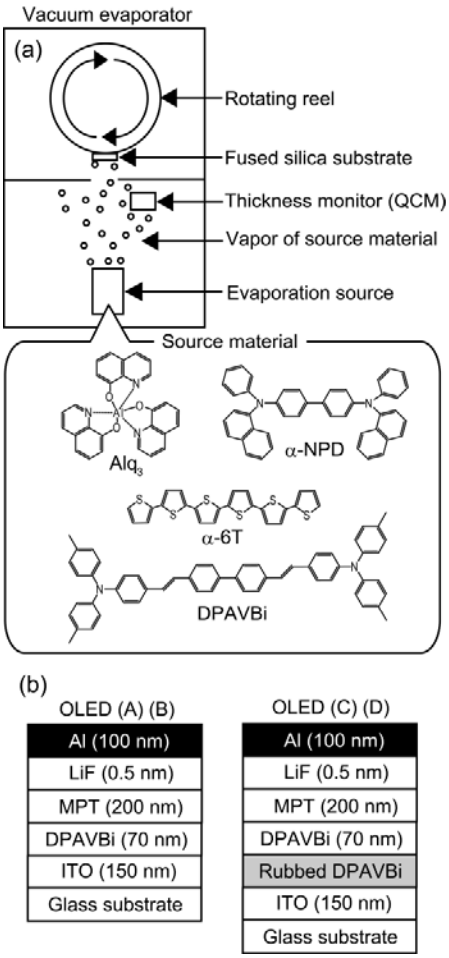

Fig. 1

T. Matsushima and H. Murata

Organic Electronics

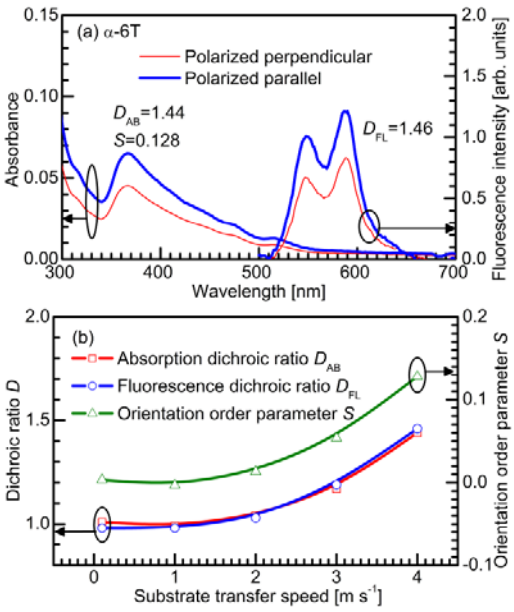

Fig. 2

T. Matsushima and H. Murata

Organic Electronics

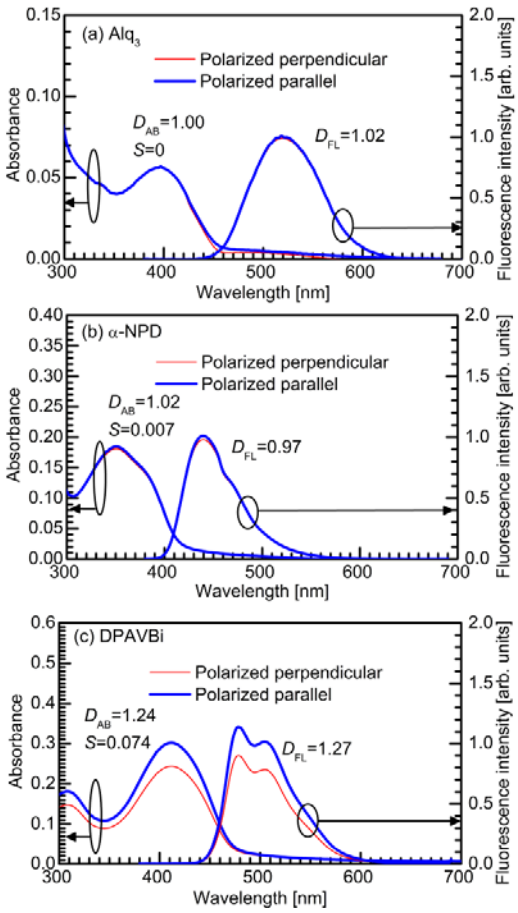

Fig. 3

T. Matsushima and H. Murata

Organic Electronics

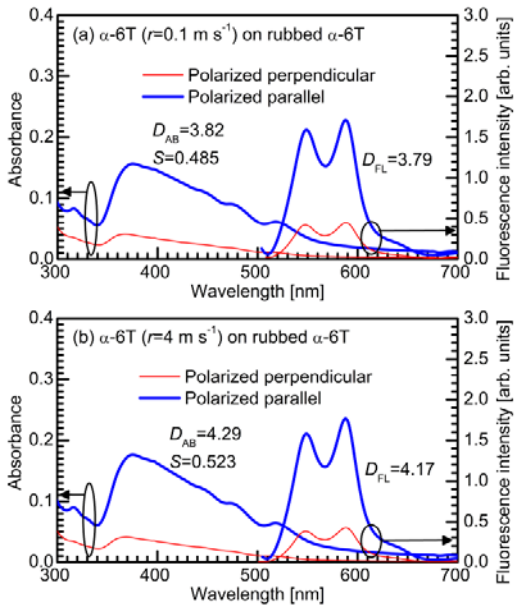

Fig. 4

T. Matsushima and H. Murata

Organic Electronics

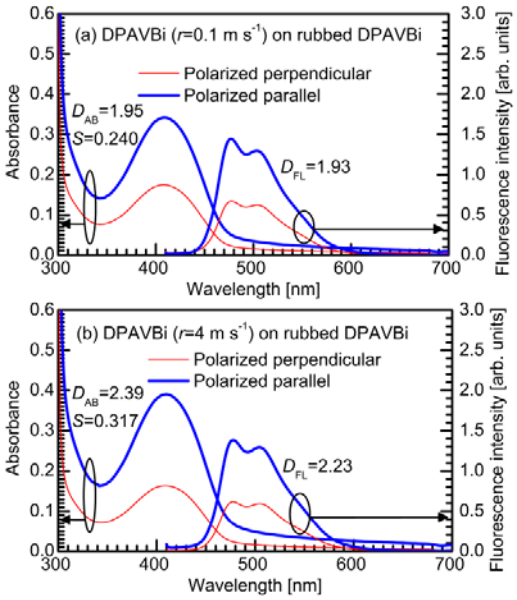

Fig. 5

T. Matsushima and H. Murata

Organic Electronics

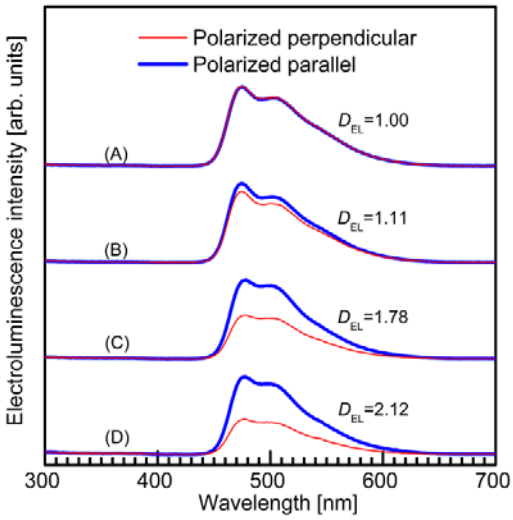

Fig. 6

T. Matsushima and H. Murata

Organic Electronics